Adsorption Behavior of Basic Dyes on Activated Clay

Yung-Chien Hsu[a]; Chun-Chiao Chiang[a]; Mei-Feng Yu[a]
[a] DEPARTMENT OF CHEMICAL ENGINEERING, NATIONAL TAIWAN INSTITUTE OF TECHNOLOGY, TAIPEI, REPUBLIC OF CHINA

PLEASE SCROLL DOWN FOR ARTICLE

Adsorption Behavior of Basic Dyes on Activated Clay

YUNG-CHIEN HSU,* CHUN-CHIAO CHIANG,
and MEI-FENG YU
DEPARTMENT OF CHEMICAL ENGINEERING
NATIONAL TAIWAN INSTITUTE OF TECHNOLOGY
43 KEELUNG ROAD, SECTION 4, TAIPEI, 106, REPUBLIC OF CHINA

ABSTRACT

Activated clay was used to study the adsorption behavior of dyestuffs in synthetic wastewater containing dyestuffs. Three basic dyes were used: C.I. Basic Red 18 (or BR18), C.I. Basic Red 46 (BR46), and C.I. Basic Yellow 28 (BY28). Adsorption occurred almost instantaneously upon contact. The mechanism of adsorption was explained by a charge to the electrostatic attractive force described in the Langmuir adsorption isotherm. The mass transfer coefficient was also calculated by the external mass transfer model in an adsorbent according to Mckay et al. Parameters including species of basic dyes, initial concentration, temperature, size of adsorbent, and NaCl were extensively investigated.

Key Words. Adsorption; Activated clay; Wastewater; Basic dye; Mass transfer

1. INTRODUCTION

The dyeing and finishing industries often discharge deep colored wastewater which has been treated by chemical coagulation, biotreatment after dilution, or the oxidation-reduction process. Active carbon may also be used. Generally speaking, biotreatment by microorganisms is not particularly effective due to poor biodegradability with poor biosorption. Active carbon is effective but it is costly and its regeneration is no simple task.

* To whom correspondence should be addressed.

2513

Investigators are more interested in low-cost adsorbents such as silica gel (1, 2), sawdust (3), and bagasse (4). Gupta et al. (5) used coal and fly ash to decolor the dye's wastewater. Economic consideration has always been a big factor in wastewater treatment.

Mckay et al. (6, 7) studied the external mass transfer coefficients of the adsorbents, and derived an equation (8) through dimensional analysis to describe the porous diffusivity with respect to time. The amount of adsorbate was reported to be directly proportional to the square root of time. The adsorption is also affected by the electrophoretic mobility that is highly pH-dependent (9, 10). Activated clay has been used with satisfactory results to treat high strength wastewater containing emulsified fatty acids (11). We attempt in this work to investigate further its adsorption behavior in treating dyeing wastewater.

Activated clay is a porous matrix containing oxides of silicon and aluminum. It is often manufactured from acidic medium at pH 2–3. The pH values may vary slightly with the quantity of activated clay used. Activated clay is inexpensive and has been widely used in the decoloration process by the cooking oil industry. However, its use for the adsorption of dyes in aqueous solution has not been well documented. Wu et al. (12) reported that basic dye C.I. Basic Blue 69 can specifically be adsorbed onto activated clay. Whether the results are also valid for other basic dyes needs further investigation. Moreover, the equation $C_t/C_0 = A + B \log(t)$, proposed by Wu et al. (12) for calculation of the external mass transfer coefficient, becomes infinite at the limit $[d(C_t/C_0)/dt]_{t=0}$. This drawback has to be overcome.

This work was therefore undertaken not only to investigate the adsorption behavior for the basic dyes BR18, BR46, and BY28, but also to propose an equation for the calculation of the external mass transfer coefficients. The coefficients calculated from this equation are compared with the literature data.

2. THEORETICAL

The adsorption of dye molecules onto activated clay in aqueous solution occurs in a liquid–solid system. The parameters that affect the adsorption include the specific surface areas, the characteristics and sizes of the adsorbent particles, and the functionality of the adsorbate.

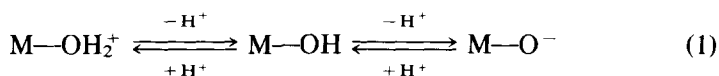### 2.1. Adsorption by the Activated Clay

The major composition of activated clay consists of SiO_2 and Al_2O_3 as illustrated in Table 1 (13). In addition to the Si/Al ratio, its adsorptability

TABLE 1
The Components of Activated Clay[a]

SiO$_2$	Al$_2$O$_3$	MgO	CaO	Fe$_2$O$_3$	K$_2$O + Na$_2$O	Loss on ignition
67–75	15–20	2.5	0.5	2.0	0.8	<10

[a] Expressed in wt%.

is also affected by the pH of the solution. The surface charge of aluminum silicate changes with the acidity (or the basicity) (14), which will result in different degrees of adsorbability. Protonation and deprotonation present different charged species of functionality on the surface (15) as revealed by Eq. (1):

$$M\text{—}OH_2^+ \underset{+H^+}{\overset{-H^+}{\rightleftharpoons}} M\text{—}OH \underset{+H^+}{\overset{-H^+}{\rightleftharpoons}} M\text{—}O^- \tag{1}$$

where M denotes Al or Si atoms in activated clay.

The isoelectric point, pI, is reached when no net charge exists on the surface of activated clay. When pI < pH, the surface bears a net negative charge and tends to attract positively charged particles (the basic dyes), and vise versa when pI > pH (16).

The pI values are 2 and 9 for silica and aluminum, respectively. In general, the final adsorbability depends on the Si/Al ratio of the clay. A ratio of 1–5 tends to pick up both the cations and the anions, while cationic species are attracted in a ratio range of 5–6 (17).

At pH as low as 2 (i.e., a condition of pI < pH), activated clay is still negatively charged as indicated by its negative electrophoretic mobility (18). This is favorable for adsorption of positively charged basic dyes. However, poor adsorption is expected for the negatively charged acidic dyes under the some conditions.

2.2. Adsorption Isotherm

Three models are usually used to describe the adsorption behavior: the Langmuir, the Freundlich, and the BET equations. Practically, the adsorption of basic dyes by the activated clay can be described by the Langmuir adsorption isotherm, which states

$$\frac{C_e}{q_e} = \frac{1}{K} + \frac{a}{K} C_e \tag{2}$$

where C_e is the equilibrium concentration of adsorbate in solution, q_e represents the adsorbed dye per unit mass of activated clay at equilibrium, and K and a are the Langmuir isotherm constants. A linearity can be obtained by plotting C_e/q_e vs C_e, from which the intercept $1/K$ and the slope a/K, and thus the values of a and K, are derived. The ratio K/a is defined as the capacity factor. The Langmuir model was adopted in this work.

2.3. The External Mass Transfer Coefficient

Assuming good mixing of the dye molecules and the clay particles with respect to time, mass transfer of dye molecules takes place according to the following steps:

1. The transfer of solute dyes from the bulk flow to the outer region of the liquid film on the particle (clay) surface.
2. The transfer of solute dyes through the liquid film by electrostatic attractive force as well as the diffusion mechanism onto the particle surface.
3. The transfer of solute dye molecules from the particle surface into the porous cavity.

The external mass transfer coefficient can be evaluated primarily by assuming Step 3 to be rate-limiting according to Mckay et al. (7). The equations proposed therein are discussed in the following sections.

2.3.1. The Differentiation Method (7)

The concentration variation rate of dyes in solution and the external mass transfer coefficient are related by the following equation:

$$\frac{dC_t}{dt} = -\beta S_S(C_t - C_S) \tag{3}$$

The boundary conditions are $C_t = C_0$ and $C_S = 0$ at $t = 0$. In Eq. (3), C_0 (mg/L) is the initial concentration, C_S (mg/L) is the dye concentration on the surface of activated clay, C_t (mg/L) is the concentration in the bulk solution at time t, S_S is the outer surface of adsorbent per unit volume of particle-free slurry, and β is the external mass transfer coefficient in cm/s.

Using the cited value of external surface area of the adsorbent particles (7) and the shape factor $\phi = 0.73$ (19), we derived the value of S_S from

$$S_S = \frac{6m}{\phi d_p \rho_l (1 - \epsilon_p)} \tag{4}$$

where the parameters d_p, ρ_l, ϵ_p, and m are the diameter of the particle (m), the density of the liquid (kg/m^3), the porosity of the activated clay, and the mass of activated clay per unit volume of liquid (g/L), respectively.

Substitution of Eq. (4) into Eq. (3) and taking limit $t \to 0$ yields

$$\beta = -\frac{1}{S_S}\left[\frac{dC_t/C_0}{dt}\right]_{t=0} \tag{5}$$

Using the initial three sets of data, we propose the following approximation by the exponential law:

$$C_t/C_0 = Ae^{-\alpha t} \tag{6}$$

where A and α are constants for the different initial concentrations of dye solution.

By differentiating Eq. (6) and setting $t = 0$, we obtained $[(dC_t/C_0)/dt]_{t=0}$. The value of β in Eq. (5) can be determined from the initial slope of plotting C_t/C_0 vs t.

2.3.2. The Integration Method (7)

According to Mckay et al. (7), we have

$$\ln\left[\frac{C_t}{C_0} - \frac{1}{1 + m_S K}\right] = \ln\left[\frac{m_S K}{1 + m_S K}\right] - \left[\frac{1 + m_S K}{m_S K}\beta S_S t\right] \tag{7}$$

where K is the adsorption constant and m_S is the mass of activated clay per unit volume of dye-free particle. The value of K can be derived by using the Langmuir model as discussed in Section 2.2. The slope $[-(1 + m_S K)\beta S_S t/m_S K]$ can be obtained by plotting $\ln\{(C_t/C_0) - [1/(1 + m_S K)]\}$ vs t. Since the value of S_S was readily obtained from Eq. (4), the external mass transfer coefficient β can thus be determined, provided that the values of K and m_S are given.

3. MATERIALS AND METHODS

3.1. Experimental Apparatus

As sketched in Fig. 1(A), the agitation apparatus was made of acrylic resin. The external basin (20 cm $\times$ 20 cm) serves as a jacket into which water from a thermostatic water bath constantly flows. The inner chamber, serving as a stirred tank, is a cylindrical container of size $T \times D_i \times H = 0.4$ cm $\times$ 10 cm $\times$ 20 cm. Inside the cylindrical inner chamber, eight pieces of baffle ($W \times L = 1$ cm $\times$ 20 cm) are evenly installed on the inside wall. A six-blade stainless steel turbine (Fig. 1B) was used as
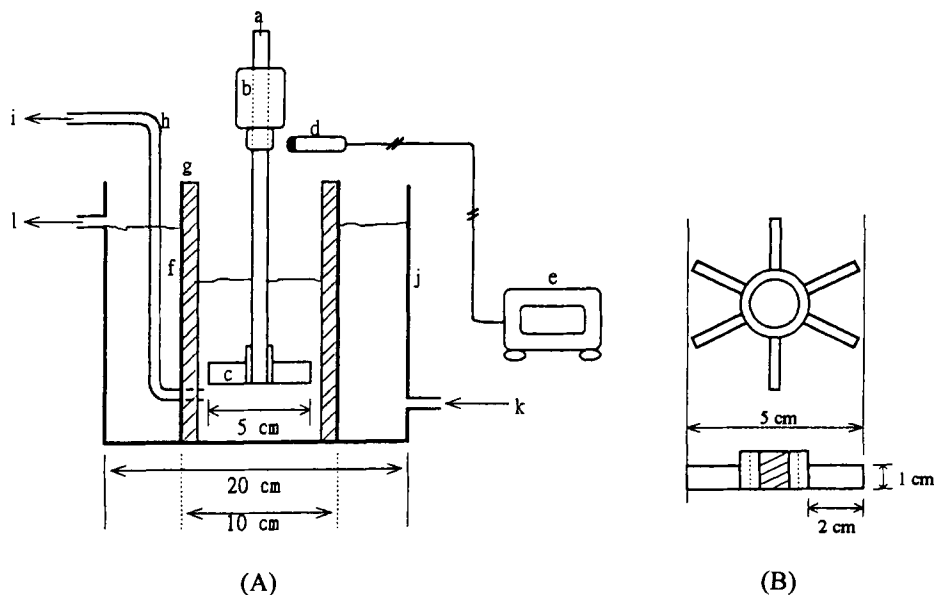
FIG. 1 Agitation unit. (A) Agitation apparatus. (B) Six-blade impeller. (a) Shaft, (b) variable speed motor, (c) six-blade impeller, (d) speed sensor, (e) speed indicator, (f) agitation tank, (g) baffle, (h) sampling tube, (i) sampling nozzle, (j) jacket, (k) water input, (l) water outlet.

the stirrer. Samplings were performed by using a 20-mL plastic syringe to suck the sample liquid rapidly at the sampling port. Thermometers (not shown here) were used both inside and outside of the stirred chamber for temperature measurements.

3.2. Chemicals

Three basic dyes [C.I. Basic Red 18 (BR18), C.I. Basic Red 46 (BR46), and C.I. Basic Yellow 28 (BY28)] were provided by Taiwan I-Hwa Co. and Bayer Chemical Co. (Germany).

Hydrochloric acid (35%) was manufactured by Hayashi Pure Chemical Industries Ltd. NaOH (96%) was supplied by Nacali Tesque Ltd. Sodium chloride (>99.5%) was a product of Tung-Hsiao Sodium Chloride Co.

The RO water was prepared by a Barnstead RO pure ST (Reverse Osmosis water system + NANO pure, Deionization Ultrapure System) with

a specific resistance larger than 18.0 MΩ-cm. The activated clay (size, 38 $\pm$ 10 μm) was purchased from Laporte Industries (Singapore) Pte., Ltd.

3.3. Instrumentation

The acetyl cellulose filter membrane was a product of Micro Filtration System with a pore size of 0.45 μm and an outer diameter of 25 mm. It was placed in a filter with a diameter of 25 mm, provided by Gelman Co. The sampler was a 20-mL syringe, a product of Taiwan Top Co. It sampled the dye wastewater at regular intervals. A circulating bath provided by Julabo Labertechnik GMBH Co. (Type F10-UC) was maintained at a constant temperature to control the temperature of the agitated tank to a precision of ± 0.1°C in the 20–100°C range. The specific surface area and the porosity of the clay were determined by a BET, a product of Micromeritics Co. (Type ASAP 2000). A plate heater with stirrer, manufactured by Corning Co. (Model PC-320, 120 V AC, 575 W, 50/60 Hz), was used as a stirrer in this experiment. The pH values were measured by a pH meter, a product of AI-ON Co. (Type MP 1800). A motor with a revolution speed range of 0–1000 rpm was provided by Hsiang Tai Co. (Type DC-2RTM). The revolution speed was measured by an IR detector type manufactured by Saint-Wien Enterprise Inc. Ltd. (Type PM490R4B30). The size of adsorbent was screened and sieved by a vibrating sieve, a product of RETSCH Co. (Type VIBRO, 110 V, 430 W, 60 Hz). The maximum absorption of dyes was measured by a spectronic 1201 UV/Vis spectrophotometer, a product by Miltron Roy Co.

3.4. Methods

3.4.1. Synthetic Wastewater

Synthetic wastewater was prepared by placing dyestuffs in RO water. The pH value was adjusted to 3.0 with HCl at 30°C.

3.4.2. The Maximum Adsorption

The three basic dye solutions were filtered and then properly adjusted to a concentration suitable for optical density measurements, and the calibration curves were established for each individual dyestuff.

3.4.3. Procedures

Dye solutions of double strength were prepared in the RO water to make 500 mL of solutions at pH 3.0, which were maintained at a desired temperature prior to the experiment (Solution A).

Activated clay of size 38 ± 10 μm, which had been placed in an oven (120°C) for more than 24 hours, was accurately weighed in double strength for a required amount and was placed in the stirring chamber containing 400 mL of RO water with pH adjusted to 3.0, and the temperature was preset to a desired value (Solution B).

Before mixing, 100 mL of Solution A was drawn for the measurement of the initial dye concentration, while the remaining 400 mL was immediately decanted into Solution B for the adsorption experiment.

At intervals of 0.5, 1, 2, 5, 30, 60, and 120 minutes, about 2 mL of the sample was drawn using a 20-mL syringe. It was then filtered through a membrane filter. The filtrate was diluted at the beginning to a proper concentration for optical measurement because of the high strength of the dye solution.

To study the effect of such experimental parameters as the agitation speed, the initial dye concentration, the particle size of activated clay, the quantity of clay used, and the temperature, we proceeded by changing one parameter at a time while holding the others constant.

4. RESULTS AND DISCUSSION

4.1. Effect of Agitation Speed on Adsorption

Figure 2 shows that the adsorption rate stayed about the same regardless of changes in agitation speed above 200 rpm, which is consistent with a previously reported result (12). This result implies that the transfer of solute on the particle surface is not affected by film thickness. However, pore diffusion turned out to be a major limiting factor (15). Liquid film diffusion on the external particle surface was caused mainly by the electrostatic attractive forces between the negatively charged activated clay and the positively charged basic dye molecules. An agitation speed of 500 rpm was selected for all our experiments to secure thorough mixing.

4.2. Effect of the Quantity of Activated Clay on Adsorption

The fact that only a very small amount of adsorbent clay was present in the 1 g/L experiment in Fig. 3 indicated random adsorption. We suspect it was a result of the adsorption site on the activated clay adsorbing the basic dye (BR18) molecules.

The adsorption curve became rather steady with 2 g/L of clay present. However, the adsorbability diminished as the amount of clay was increased. The amount of dyes adsorbed per unit mass of clay decreases with an increasing amount of clay added. Such a phenomenon is similar
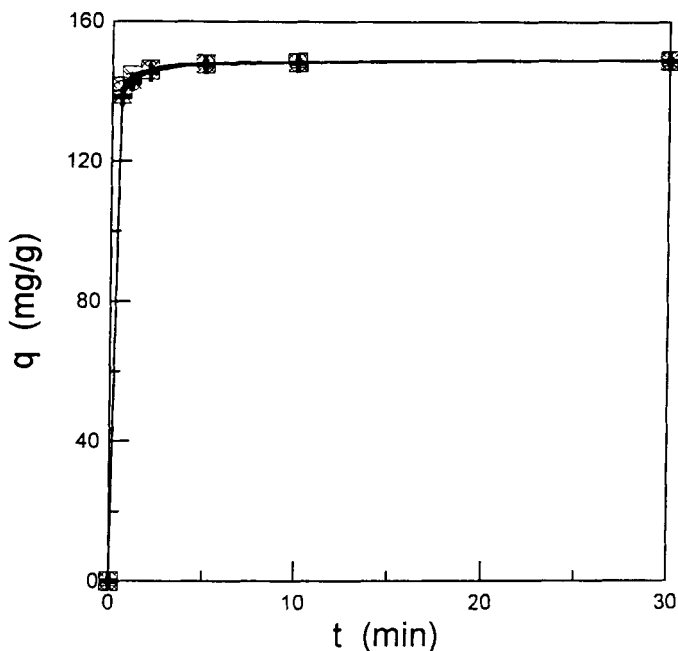
FIG. 2   Effect of agitation speed on adsorption capacity for BR18. Temperature = 30°C, pH 3, 0 < d_p ≤ 38 μm, activated clay = 2g/L, C_0 = 300 mg/L, (+) 200 rpm, (△) 300 rpm, (*) 400 rpm, (⊠) 500 rpm, (○) 600 rpm.

to that of instantaneous adsorption (20, 21). It is also consistent with the results of Giles et al. (22), who classified such a high affinity as an H-type adsorption. Experiments with other basic dyes such as BY28 and BR46 found similar characteristics (not shown here). 2 g/L of activated clay was used throughout the following experiments of this work.

4.3. Effect of Particle Size on Adsorption

The adsorption surface area is highly dependent on the particle size, which in turn affects the adsorption rate as well as the adsorption capability. The specific surface areas are 147.33, 99.51, 89.87, and 87.68 m²/g for particle sizes of <38, 38–63, 63–75, and 75–106 μm, respectively, among which the group with size <38 μm showed the best result for BR18 (Fig. 4). Similar results were also observed for BR46 and BY28 (data not shown
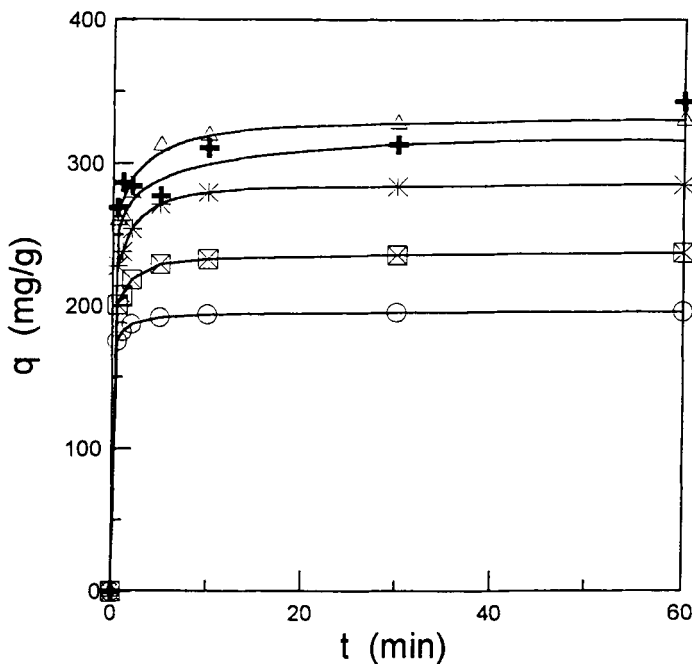
FIG. 3   Effect of activated clay concentration on adsorption capacity for BR18. Temperature = 30°C, rpm = 500, pH 3, $0 < d_n \leq 38$ μm, $C_0 = 700$ mg/L, (+) activated clay = 1 g/L, (△) activated clay = 2 g/L, (*) activated clay = 3 g/L, (⊠) activated clay = 4 g/L, (○) activated clay = 5 g/L.

here). It was found that the larger the specific surface area, the greater the adsorption capability and the more rapid the adsorption rate are, a result in good agreement with the cited references (15, 18).

4.4. Adsorption Isotherm

Figure 5 was obtained by plotting the adsorption capacity of BR18 dye, as an example, versus time to show that the adsorption rate is rather high. This was caused by strong attractive forces between the dye molecules and the clay, fast diffusion onto the external surface that was followed by fast pore diffusion into the intraparticle matrix to attain rapid equilibrium. It was observed that the higher the initial dye concentrations, the higher adsorbate per unit adsorbent mass. Similar results were found for
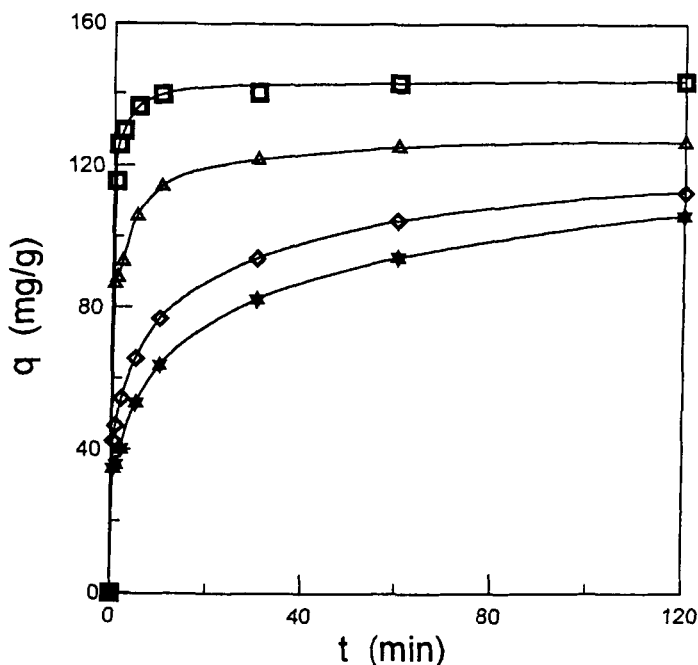
FIG. 4   Effect of particle sizes on adsorption capacity for BR18. Temperature = 30°C, rpm = 500, activated clay = 2 g/L, pH 3, C_0 = 300 mg/L, ($\square$) $0 < d_p \leq 38$, ($\triangle$) $38 \leq d_p \leq 63$, ($\diamond$) $63 \leq d_p \leq 75$, ($\star$) $75 \leq d_p \leq 106$.

BR46 and BY28 (not shown here) that agree with the literature (20). At low initial concentration (e.g., less than 110.56 mg/L), instantaneous adsorption occurred without significant lag time (Fig. 5). The Langmuir model is well fitted when we plotted C_e/q_e vs C_e for the three dye species (Fig. 6), which is consistent with the literature (18, 20). The a, K, and K/a values, as reported in Table 2, were calculated using the Langmuir adsorption isotherm. Of the three, dye BR18 has the greatest capacity factor.

4.5. Effect of Sodium Chloride on Adsorption

In the dye manufacturing process, NaCl is usually discharged into the wastewater for its salting-out effect.
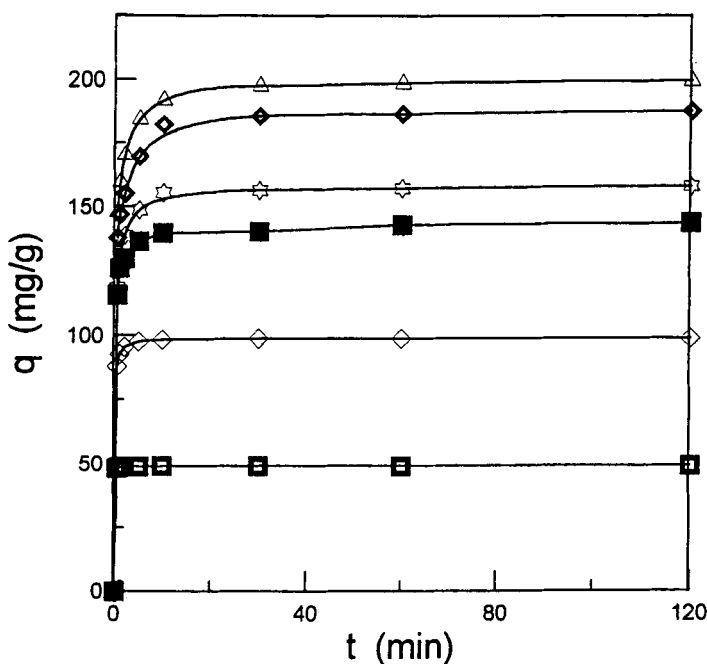
FIG. 5   Effect of initial concentration of dyes on adsorption capacity for BR18. Temperature = 30°C, rpm = 500, pH 3, $0 < d_p \leq 38$ μm, activated clay = 2 g/L, ($\square$) C_0 = 110.56 mg/ L, ($\diamondsuit$) C_0 = 213.53 mg/L, ($\blacksquare$) C_0 = 326.16 mg/L, ($\star$) C_0 = 366.76 mg/L, ($\diamondsuit$) C_0 = 443.29 mg/L, ($\triangle$) C_0 = 519.83 mg/L.

In our experiment we noticed that the presence of NaCl greatly enhanced the adsorption capability of activated clay (Fig. 7). We think that in the presence of NaCl, an electrolyte, the charge density in the diffusion layer is significantly increased, which in turn minimizes the volume of diffusion layer required to neutralize the surface charge. Sodium cation has a thinning effect on the diffusion layer formed on the surface of the particles. Although the total net charge did not change, the thickness of the diffusion layer had diminished significantly (15). The enhancement of adsorption caused by NaCl has also been documented (18, 23).

Similar results with little discrepancy were obtained for BR18 and BY28 (not shown here). The differences in the molecular structures of the dyes may have contributed to any discrepancy.
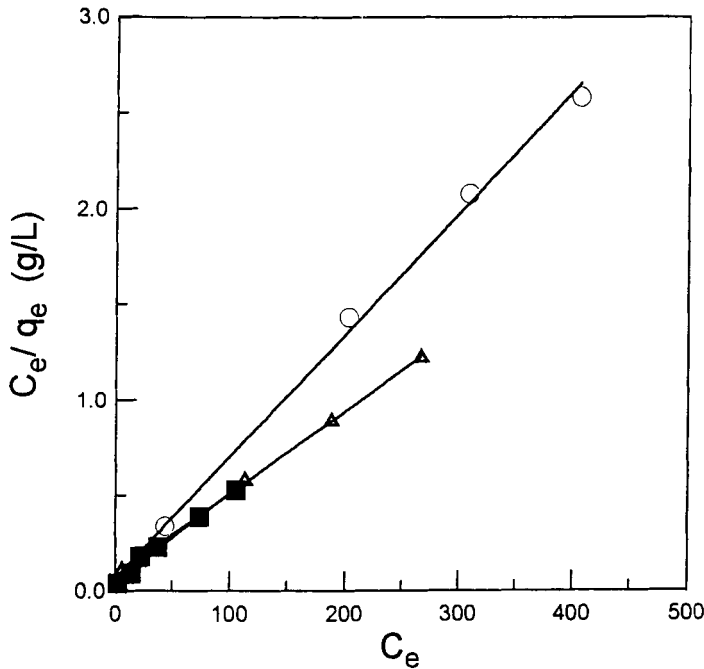
FIG. 6   A plot of the Langmuir adsorption isotherm for dyes. Temperature = 30°C, rpm = 500, pH 3, $0 < d_p \leq 8$ μm, activated clay = 2 g/L, (■) BR18, (○) BR46, (△) BY28.

4.6. Effect of Initial Dye Concentration on Intraparticle Diffusion

Plotting the amount adsorbed, q, vs $t^{1/2}$ from the adsorption of BY28 reveals a two-section linearity. The higher the dye concentration, the

TABLE 2
Langmuir Equilibrium Constant

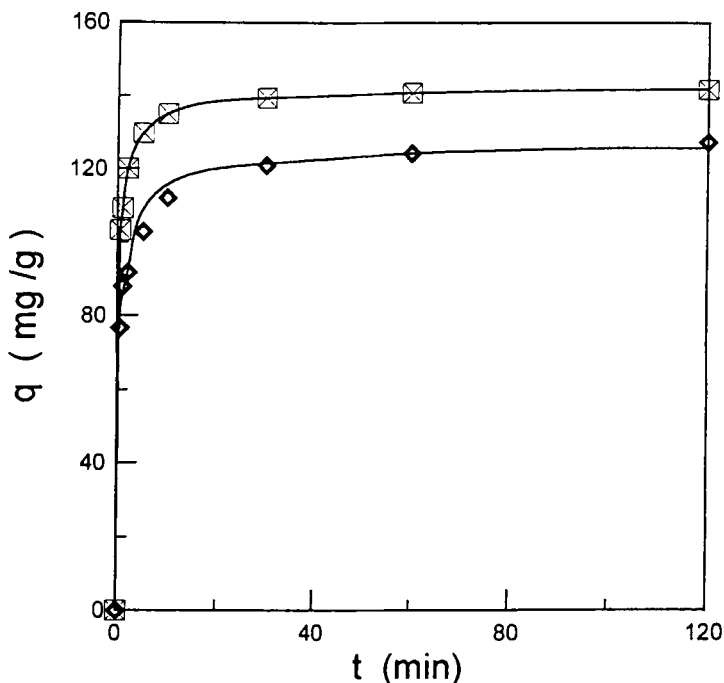| Dye	Particle size range (μm)	Temperature (°C)	Langmuir constant a (cm^3/g)	Equilibrium constant K (cm^3/g)	Capacity factor K/a (g dye/g clay)
BR18	$0 < d_p \leq 38$	30	8.01	26.35	3.29
BR46	$0 < d_p \leq 38$	30	16.02	10.37	0.65
BY28	$0 < d_p \leq 38$	30	18.67	12.48	0.67

FIG. 7   Effect of NaCl on adsorption capacity for BR46. Temperature $= 30°C$, rpm $= 500$, pH 3, $0 < d_p \leq 38$ μm, activated clay $= 2$ g/L, $C_0 = 300$ mg/L, (◊) without NaCl, (⊠) 1 g NaCl/L added.

higher the adsorption rate, and the more efficient adsorption became with respect to the adsorption capacity q. In Fig. 8 we see three different adsorption stages taking place. The first or instantaneous stage (as shown by dotted lines) may be related to electrostatic attraction between the dye cations and the surface anions of the clay. A similar instantaneous stage relating the adsorption of methylene blue onto montmorillonite clay was reported by Sethurama and Raymahashay (21). At the second stage the dyes adsorbed on the surface of the clay, or remaining in the bulk solution, diffused into pores of the clay. As the initial concentration of dye wastewater is increased, the adsorption lines slope upward. This is due to the greater driving force of dye between the bulk and the surface of the particles as well as the pores. This fact may be attributed to intraparticle diffusion of the dye molecules, and it agrees with Mckay's result concerning
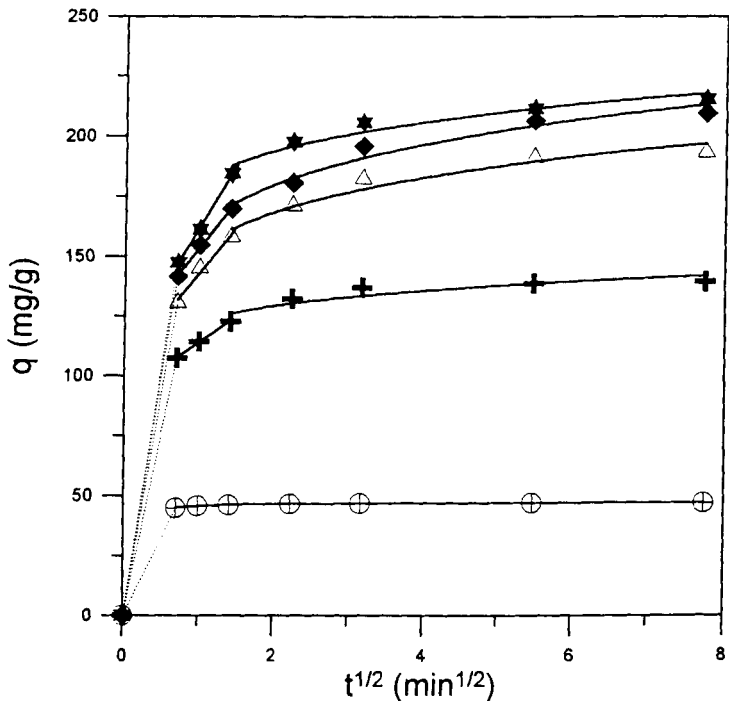
FIG. 8   A plot of q vs $t^{1/2}$ for BY28 at various initial concentrations. Temperature $= 30°C$, rpm $= 500$, pH 3, $0 < d_p \leq 38$ μm, activated clay $= 2$ g/L, ($\oplus$) $C_0 = 99.84$ mg/L, ($+$) $C_0 = 299.18$ mg/L, ($\triangle$) $C_0 = 504.79$ mg/L, ($\blacklozenge$) $C_0 = 629.98$ mg/L, ($\star$) $C_0 = 704.74$ mg/L.

the adsorption of dye onto the active carbon (8). At the final stage, almost all active sites of the activated clay are occupied by dye molecules, and adsorption reaches the equilibrium state.

4.7. External Surface Mass Transfer Coefficient

Two methods were used to determine the external surface mass transfer coefficient: The differentiation method and the integration method.

4.7.1. The Differentiation Method

As shown in Fig. 9, the adsorption rates for BY28 were found to be lower at higher initial concentrations. They gradually increased as the
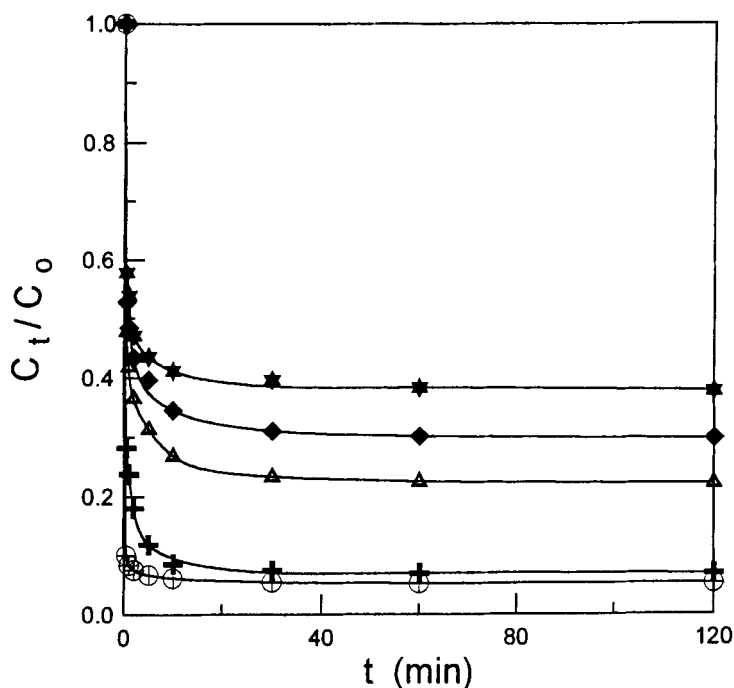
FIG. 9   Effect of initial concentration on the adsorption rate for BY28. Temperature = 30°C, rpm = 500, pH 3, 0 < d_p ≤ 38 μm, activated clay = 2 g/L. (⊕) C_0 = 99.84 mg/L, (+) C_0 = 299.18 mg/L, (△) C_0 = 504.79 mg/L, (◆) C_0 = 629.98 mg/L, (★) C_0 = 704.74 mg/L.

concentrations were lowered. The effect of initial concentration on the adsorption rate was evident. The result depends on the characteristics of the basic dyes. The external surface mass transfer coefficients, as obtained by using the differentiation method according to Mckay et al. (6) (Table 3), decrease with an increase in initial concentrations. However, the discrepancy in the order of magnitude between Mckay's (7) and our work may be a result of using different values for the properties of chemical species, including the electrostatic attractive forces, the particle sizes (150–1000 vs 38 μm), and the shape factors [φ = 1 (7) vs 0.73 (19)]. The difference could be minimized by using the same set of properties. As a result, the orders of β become comparable, and the β values approach the literature values. Similar results were observed for BR18 and BR46 (data not shown here). The β values obtained by the differential method

TABLE 3
Effect of Initial Concentration and Temperature of the Dye Solution on Surface Mass
Transfer Coefficient Evaluated by the Differentiation Method[a]

Temperature (°C)	C_0 (mg/L)	β (cm/s)		
		BR18	BR46	BY28
30	100	1.98×10^{-5}	1.76×10^{-5}	1.40×10^{-5}
30	200	1.67×10^{-5}		
30	300	1.27×10^{-5}	6.76×10^{-6}	1.00×10^{-5}
30	350	9.98×10^{-6}		
30	450	7.73×10^{-6}		
30	500	7.53×10^{-6}	4.50×10^{-6}	6.59×10^{-6}
30	600		3.75×10^{-6}	5.56×10^{-6}
30	700		3.49×10^{-6}	4.80×10^{-6}
10	300	1.11×10^{-5}	5.34×10^{-5}	1.00×10^{-5}
20	300	9.26×10^{-6}	7.14×10^{-5}	1.03×10^{-5}
45	300	1.00×10^{-5}	6.82×10^{-5}	1.04×10^{-5}

[a] rpm = 500, activated clay = 2 g/L, $0 < d_p \leq 38$ μm, pH 3.

under different initial concentrations and temperatures of dye solutions are presented in Table 3.

4.7.2. The Integration Method

The integration method, as proposed by Mckay et al. (7), was considered more accurate for evaluating the external surface mass transfer coefficient. According to Eq. (7), a plot of $\ln\{(C_t/C_0) - [1/(1 + m_S K)]\}$ vs t gives Fig. 10. By taking the limit $t \to 0$, we obtained the slope $[- (1 + m_S K) \beta S_S t / m_S K] \beta S_S$, from which the values of β were determined by substituting the values of K, S_S, and m_S. Similar calculations were performed for the other two dye species. β values are listed in Table 4. The results in Tables 3 and 4 are comparable.

4.8. Effect of Temperature on Adsorption

The wastewater from a dyeing and finishing plant is generally discharged without cooling. The wastewater temperature affects the adsorption rate as well as the adsorption capacity. In some cases its effect is positive while in others it is negative (15).

A plot of the amount of BR46 adsorbed per unit mass in the activated clay vs time (Fig. 11) shows that the temperature effect is rather signifi-
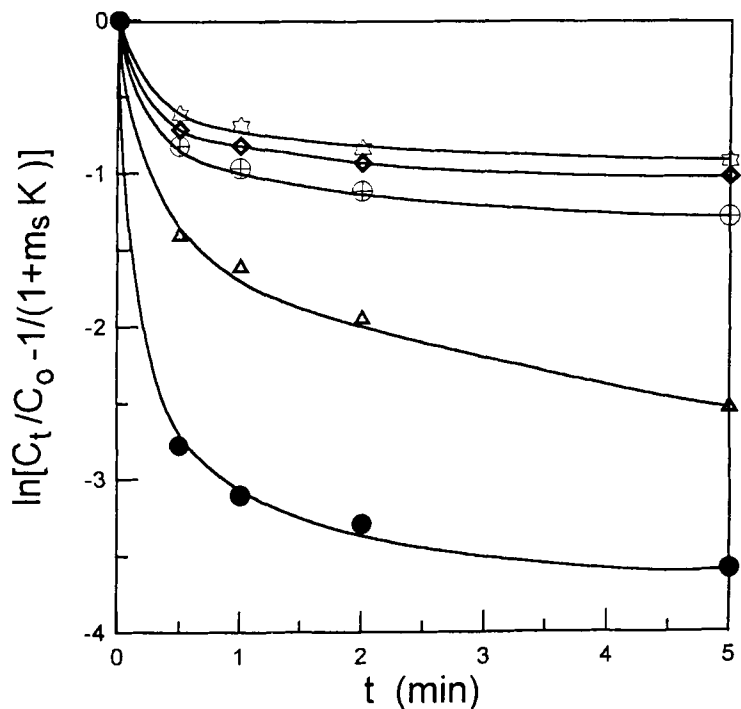
FIG. 10   A plot of $\ln[C_t/C_0 - 1/(1 + m_sK)]$ vs t for BY28. Temperature $= 30°C$, rpm $=$ 500, pH 3, $0 < d_p \leq 38$ μm, activated clay $= 2$ g/L, (●) $C_0 = 99.84$ mg/L, (△) $C_0 = 299.18$ mg/L, (⊕) $C_0 = 504.79$ mg/L, (◇) $C_0 = 629.98$ mg/L, (☆) $C_0 = 704.74$ mg/L.

TABLE 4
Effect of Initial Concentration on Surface Mass Transfer Coefficient Evaluated
by the Integration Method[a]

C_0 (mg/L)	β (cm/s)		
	BR18	BR46	BY28
100	6.91×10^{-5}	5.95×10^{-5}	4.47×10^{-5}
200	3.79×10^{-5}		
300	2.57×10^{-5}	1.30×10^{-5}	2.27×10^{-5}
350	1.96×10^{-5}		
450	1.65×10^{-5}		
500	1.56×10^{-5}	1.00×10^{-5}	1.33×10^{-5}
600		8.78×10^{-6}	1.15×10^{-5}
700		8.47×10^{-6}	9.97×10^{-6}

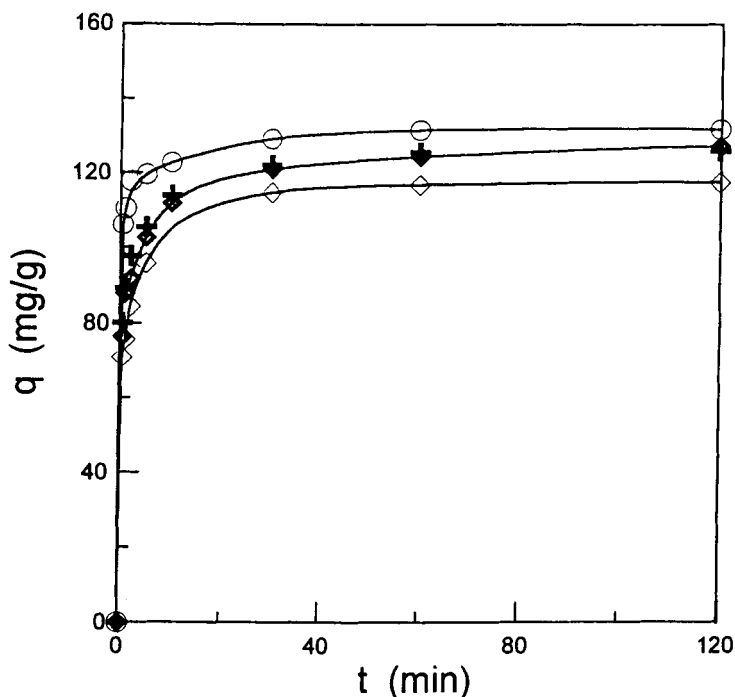[a] Temperature $= 30°C$, rpm $= 500$, activated clay $= 2$ g/L, $0 < d_p \leq 38$ μm.

FIG. 11   Effect of temperature on adsorption capacity for BR46. C_0 = 300 mg/L, rpm = 500, pH 3, 0 < d_p ≤ 38 μm, activated clay = 2 g/L, (O) temperature = 10°C, (+) temperature = 20°C, (◊) temperature = 30°C, (◊) temperature = 45°C.

cant. Similar results were observed for BY28 and BR18, although they are not as significant as for BR46. Our result shows that lower temperatures facilitate adsorption, which is in agreement with the cited reference (15). The result follows the Arrhenius equation, i.e., $\beta = Ae^{-(E/RT)}$. Plotting ln β vs 1/T yields the activation energies 2.11, 4.23, and 0.65 kJ/mol for BR18, BR46, and BY28, respectively.

A value below 12 kJ/mol has been considered as an indication of physical adsorption. The degree of temperature effect on the adsorption of the different basic dyes by activated clay varies from species to species, attributable to structural distinctions. The physical adsorption of dye molecules onto activated clay is inherently a reversible process. At high temperatures the increased kinetic energy enhances the molecular mobility, causing a greater degree of desorption, and hence lower adsorption. Moreover, the data in Fig. 11 at 20 and 30°C are very close, possibly due to

experimental errors or some unknown causes that need to be investigated further.

5. CONCLUSION

Three basic dyes were tested for their adsorption behavior onto activated clay. Activated clay showed excellent affinity for the basic dyes. The adsorption is a physical phenomenon. Degree of adsorbability depends greatly on the species of basic dyes, temperature, and relative concentrations of the adsorbate and the adsorbent. Sodium chloride contained in the wastewater exerts a positive effect on the adsorption.

The adsorption behavior can be successfully described by the Langmuir isotherm, while the external surface mass coefficient, as calculated according to Mckay et al., is consistent with values cited in the literature. Three stages of adsorption were adopted to describe the adsorption phenomena of basic dyes onto activated clay. The adsorption of basic dyes onto activated clay took place almost instantaneously. The higher the initial dye concentration, the higher the adsorption rate. Moreover, the adsorption capacity of activated clay was comparatively high, and hence it seems to be a potential adsorbent for dye manufacturing wastewater. Of course, its feasibility will depend on the solution of secondary pollution problems. The current view aims at reusing the used activated clay, possibly as raw material in manufacturing cement.

NOMENCLATURE

A constant in Eq. (8)

a constant in Langmuir isotherm (cm^3/g)

C concentration of dye (mg/L)

C_0 concentration of dye in bulk liquid at $t = 0$ (mg/L)

C_e concentration of dye at equilibrium (mg/L)

C_s concentration in liquid at outer surface of particle (mg/L)

C_t concentration of dye in bulk liquid at time t (mg/L)

d_p particle diameter (μm)

K constant in Langmuir isotherm (cm^3/g)

m concentration of activated clay in liquid volume (g/L)

M mass of dye (g)

m_S mass of activated clay per unit volume of particle-free dye (mg/L)

q solid phase dye concentration (mg/g)

q_e adsorbed dye per unit mass of activated clay at equilibrium (mg/g)

S_S outer surface of adsorbent per unit volume of particle-free slurry (cm^{-1})

t time (min)

T temperature (K)

x mass of dye removed by adsorption (mg)

Φ shape factor (—)

α constant in Eq. (8)

β surface mass transfer coefficient (cm/s)

ρ_t density of liquid (g/cm^3)

ϵ_p porosity of activated clay (—)

REFERENCES

1. F. Alexander and G. Mckay, *Chem. Eng. J.*, p. 243 (1977).
2. F. Alexander, V. J. P. Poots, and G. Mckay, *Ind. Eng. Chem., Process Res. Dev.*, *17*, 406 (1978).
3. V. J. P. Poots, G. Mckay, and J. J. Healy, *J. Water Pollut. Control Fed.*, p. 926 (May 1978).
4. G. Mckay, M. E. Geundi, and M. M. Massar, *Water Res., 21*, 1513 (1987).
5. G. S. Gupta, G. Prasad, and V. N. Singh, *Ibid., 24*, 45 (1990).
6. G. Mckay, M. E. Geundi, and M. M. Massar, *Ibid., 22*, 1527 (1988).
7. G. Mckay, S. J. Allen, I. F. Mcconvey, and M. S. Otterburn, *J. Colloid Interface Sci., 80*, 323 (1981).
8. G. Mckay, *J. Chem. Tech. Biotechnol., 33A*, 196 (1984).
9. B. Alince and P. Lepoutre, *Tappi J., 66*, 101 (1983).
10. K. K. Panday, G. Prasad, and V. N. Singh, *J. Chem. Tech. Biotechnol., 34A*, 367 (1984).
11. Y. C. Hsu, "The Method for Removing Fatty Acid from the Wastewater with High-Strength Emulsified Fatty Acid," ROC Patent 59494 (1992).
12. F. C. Wu, Y. C. Hsu, and R. L. Tseng, *J. Chin. Inst. Environ. Eng., 4*, 207 (1994).
13. Y. H. Lin, "The Study of Adsorption with Activated Clay to Treat the Wastewater of High Concentrated Emulsified Fatty Acid," MS Thesis, Department of Chemical Engineering, National Taiwan Institute of Technology, Taipei, ROC, 1991.
14. G. A. Parks, *Adv. Chem. Ser., 67*, 121 (1967).
15. L. D. Benefield, J. F. Judkins, and B. L. Weand, *Process Chemistry for Water and Wastewater Treatment*, Prentice-Hall, Englewood Cliffs, NJ, 1982.
16. M. A. Anderson and A. J. Rubin, *Adsorption Inorganics at Solid-Liquid Interface*, Ann Arbor Science Publishers, Ann Arbor, MI, 1986.
17. H. A. Elliott and C. P. Huang, *Water Res., 15*, 849 (1981).
18. H. Y. Jeng, "The Mechanism and Phenomenon of Simulant Wastewater of Emulsified Fatty Acid and Dye, Textile Dyeing Treated with Activated Clay," MS Thesis, Department of Chemical Engineering, National Taiwan Institute of Technology, Taipei, ROC, 1992.
19. C. J. Geankoplis, *Transport Processes and Unit Operations*, 3rd ed., Prentice-Hall, Englewood Cliffs, NJ, 1993, p. 122.

20. Y. C. Hsu, F. C. Wu, and R. L. Tseng, *Proc. 18th Conf. Wastewater Treatment Technology*, Taiwan, 1993, p. 705.
21. V. V. Sethurama and B. C. Raymahashay, *Environ. Sci. Technol.*, *9*, 1139 (1975).
22. C. H. Giles, D. Smith, and A. Huitson, *J. Colloid Interface Sci.*, *47*, 755 (1974).
23. E. J. W. Verwey and J. T. G. Overbeek, *Theory of the Stability of Lyophobic Colloids*, Elsevier Scientific, Amsterdam, 1948.